CI&CEQ
Chemical Industry & Chemical Engineering Quarterly

Available online at
Association of the Chemical Engineers of Serbia AChE
www.ache.org.rs/CICEQ

Chem. Ind. Chem. Eng. Q. 31 (3) 239–248 (2025) CI&CEQ

DARIO BALABAN[1,2]
JELENA LUBURA[1]
PREDRAG KOJIĆ[1]

INTEGRATED NEURAL NETWORK AND ASPEN PLUS MODEL FOR ENTRAINED FLOW GASIFICATION KINETICS INVESTIGATION

[1]University of Novi Sad, Faculty of Technology Novi Sad, Novi Sad, Serbia

[2]University of East Sarajevo, Faculty of Technology Zvornik, Zvornik, Republic of Srpska, Bosnia and Herzegovina

Article Highlights

- Sensitivity analysis of gasification kinetics of different feedstocks was performed in Aspen Plus
- Process parameters and feedstock impact on efficiency and syngas composition are analyzed
- Obtained results are used for ANN development and modeling with high accuracy
- Process parameters optimization studies regarding syngas content are performed

Abstract

Entrained flow gasification is a well-established technology, however, the main obstacle in process design is the complex gasification mechanism, since numerous phenomena at extreme process conditions take place simultaneously. This study is focused on integrated thermodynamic and artificial neural network approach (ANN) for entrained flow gasification kinetics investigation. Data on 102 feedstock materials composition was used in the AspenPlus gasification simulation, where sensitivity analysis was performed for different equivalence ratios (0.1–0.7) and gasification temperature (1200–1500°C) values. For analyzed materials, an optimal equivalence ratio range exists (usually 0.3–0.4), maximizing gasification efficiency. The obtained results were used in ANN development for each output variable (syngas composition, efficiency, heating value, and carbon conversion). Matlab algorithm was used for the determination of the optimal number of neurons (1–20 range) in each ANN. High R^2 values (>0.99) for all models suggested good agreement between simulated and predicted values. Genetic algorithm-based optimization studies for maximization of hydrogen content and cold gas efficiency result in mean ER values of 0.35 and 0.41, respectively, at a temperature of 1200 °C. Yoon interpretation method was used for quantifying the relative impacts of each input variable on syngas content and gasification efficiency. The proposed approach represents a powerful tool that can facilitate the investigation of the entrained flow gasification and process design.

Keywords: syngas; optimization; simulation; machine learning.

SCIENTIFIC PAPER

UDC 662:544.4:004

Global energy production, despite an increase in renewable energy sources consumption, is still dominated by fossil fuels. Approximately one-third of global electricity production in 2022 came from renewable energy sources, while their share in total energy consumption is even lower, approaching 20% [1,2]. Taking into account the non-renewable nature of fossil fuels and intensive greenhouse gas and pollutant emissions, the energy industry is expected to shift towards cleaner energy sources (solar, wind, hydro, geothermal, biomass, etc.) [3], which is recognized and controlled by global policies [4,5]. Thus, a serious effort is made to develop new and improve the existing energy conversion technologies.

Correspondence: D. Balaban, University of Novi Sad, Faculty of Technology Novi Sad, Bulevar cara Lazara 1, 21000 Novi Sad, Serbia.
E-mail: dario.balaban@uns.ac.rs
Paper received: 30 April, 2024
Paper revised: 27 August, 2024
Paper accepted: 18 September, 2024

https://doi.org/10.2298/CICEQ240430032B

Thermochemical conversion technologies consist of the conversion of carbonaceous feedstocks into liquid, solid, or gaseous products for further production of electricity, heat, chemicals, or fuels. Among the conventional thermochemical conversion technologies (combustion, gasification, and pyrolysis) [6], gasification offers benefits in terms of high conversion efficiency [7], achievable carbon capture and cleanup of produced gas (syngas) [8], as well as polygenerative potential due to specific syngas composition [9]. The process consists of partial oxidation of carbon in the fuel in the presence of a gasifying agent, such as oxygen, air, air-oxygen mixture, steam, steam-oxygen mixture, or carbon dioxide. Produced syngas consist mainly of carbon monoxide, hydrogen, methane, carbon dioxide, and water. The solid residue consists of ash and an unconverted organic fraction of the fuel [10,11]. Overall reacting system is endothermic, where necessary energy can be provided by partial oxidation (auto-thermal gasification) or by external supply of energy (allo-thermal gasification). Considering the auto-thermal system, gasification can be seen as a sequence of three stages: drying, decomposition (devolatilization), and gasification. Overall process output depends on several factors, including operating conditions (temperature and pressure), amount and type of gasifying agent, feedstock composition, and gasification technology [11,12].

Several gasification technologies have been developed in recent years, which differ in operating conditions, feedstock material state, capacity, efficiency, and scale-up potential. Within the currently available gasification technologies, such as fixed bed and fluidized bed, entrained flow gasifiers constitute an interesting option owing to their commercial large-scale availability (technological readiness index of around 7–8), lower emissions, and their high efficiency for the production of syngas [13,14]. Complex construction and operation, problems with construction materials at high temperatures, as well as fuel specificity in terms of particle size, are compensated by high conversion efficiency, high capacity, good gas-solid contact and mixing, moderate heating value syngas, and great scale-up potential. Typical entrained flow gasification (EFG) temperature is above ash melting point, typically in the range of 1200–1500 °C, while gasification pressure is usually above 25 bar [13,15,16].

To develop and design gasification processes, a detailed investigation of process kinetics must be done, which helps determine the impact of operating conditions and feedstock material composition on outlet parameters, i.e., carbon conversion, syngas yield, and syngas composition. Thus, several different gasification models have been developed, which can be divided into kinetic rate models, thermodynamic equilibrium models, and neural network models [15]. Kinetic models provide essential information on kinetic mechanisms to describe the conversion during biomass gasification. Several studies that include kinetic models have been made, taking into account gasification reactions, heat and mass transfer, and fluid dynamics in EFG [17–24]. Thermodynamic equilibrium models are independent of gasifier design and may be more suitable for process studies on the influence of the most important process parameters. Additionally, this model requires fewer details of the system in hand. Thus, stoichiometric and non-stoichiometric equilibrium models have extensively been used for gasification purposes [25–29], especially in the domain of EFG, since the system approaches thermodynamic equilibrium at higher temperatures [15,30]. Furthermore, this approach is often implemented in Aspen Plus simulation software, which has become a standard procedure for the simulation and investigation of the gasification process. The software enables equilibrium calculations through Gibbs free energy minimization [30]. Artificial neural networks (ANN) have recently been successfully used in various areas of chemical engineering research. The concept of ANN allows for black-box modeling of large amounts of data, which can be useful in phenomenologically complex processes, such as EFG and gasification in general. Therefore, several types of research using ANN have been conducted to evaluate the performance of various gasification systems [31], optimize a given gasification process for hydrogen production [32], model biomass gasification in fluidized bed gasifiers [33] and fixed bed downdraft gasifiers [34], predict biomass gasification process parameters [35] and develop a comprehensive gasification model, taking into account wide range of inlet and outlet parameters [36]. Also, some studies have developed an integrated thermodynamic equilibrium and ANN approach, which uses equilibrium calculation results as ANN input data, while a single output variable is considered, mainly syngas heating value [37] and net energy output [38].

By using simulation software like Aspen Plus, a thermodynamic equilibrium approach can be applied for the gasification of different feedstock materials at different operating conditions. Thus, obtained data on syngas composition can be used for the development of ANN, which will take into account feedstock composition, gasifying agent type, and flowrate, as well as operating conditions, and provide outputs in the form of syngas composition, gasification efficiency, etc. This approach can be beneficial on multiple levels, since only obtained ANN models are necessary for the evaluation of gasification performance, thus providing a tool for engineers for preliminary assessment of potential plant efficiency, gasification operation

feasibility, and necessary operating conditions. Also, gasification kinetics for a given material can be assessed without the use of a process simulator, while a comparative analysis of the behavior of different feedstock materials can be performed.

It is worth mentioning that there is ongoing research and development in the field of gasification, and new and innovative technologies are emerging that could potentially surpass EFG in terms of efficiency and cost-effectiveness [39–41]. Nonetheless, EFG remains one of the most promising and widely used gasification technologies at present. Therefore, the goal of this research is to investigate in detail the kinetics of the EFG process via an integrated ANN and thermodynamic equilibrium approach. To obtain representative data on EFG, numerous different feedstock materials have been investigated, whose composition is taken from the literature and used as an input in Aspen Plus gasification simulation. Typical oxyfuel gasification process flowsheet configuration was used, while sensitivity analysis was performed for all samples, with equivalence ratio and gasification temperature as parameters to be varied. Obtained results are used as input data for ANN development using a Matlab algorithm for network topology optimization. Obtained models for the prediction of output variables (syngas composition, cold gas efficiency, carbon conversion, and syngas LHV) are further used for developing the objective function for optimization via the genetic algorithm method. The objective function uses equivalence ratio and temperature as decision variables and parameters of interest as target variables, thus allowing for quick determination of optimal process parameters for a given feedstock material.

MATERIALS AND METHODS

Feedstock material data

To develop a comprehensive gasification model, a wide range of input parameters is necessary. Since gasification is suitable for a relatively broad spectrum of raw materials, data on various feedstock material types' composition is obtained from the literature. The general idea is to obtain data on proximate and ultimate analysis for materials of different origins and heating values, providing the necessary range of individual component composition. Data on proximate and ultimate analysis is obtained for 40 municipal solid waste (MSW) and refuse-derived fuel (RDF) samples, 39 biomass samples, 10 coal samples, and 13 biomass briquettes samples. Complete input data is given in Supplementary material, Table S1. Since further calculations require the data on materials' lower heating value (*LHV*), for instances where only a higher heating value (*HHV*) is given, necessary conversion is made according to Eq. (1) [42]:

$$LHV = HHV - (9 \cdot H + Moisture) \cdot 2.44 \left[\frac{MJ}{kg}\right] \quad (1)$$

where *H* and *Moisture* stand for hydrogen and moisture content, respectively

Process simulation and sensitivity analysis

Gasification process simulation is performed in Aspen Plus software. Raw material composition data is used in the definition of nonconventional components, with HCOALGEN and DCOALIGT models being used for enthalpy and density calculations. Peng-Robinson equation of state was used as a thermodynamic model. Defined components consist of nonconventional components (raw material and ash), decomposition products (C, H_2, N_2, H_2O, S, Cl_2, O_2), and possible syngas components (CH_4, CO, CO_2, NO, NH_3, HCl, H_2S, C_2H_6). A typical gasification process flowsheet (Figure 1) is developed, where feedstock material (FEEDSTOCK) first enters the decomposition (DECOMP - Ryield) reactor, where drying and devolatilization processes take place at 500 °C and gasification pressure of 25 bar. Then, the mixture enters the gasification reactor (GASIFIER - RGibbs), along with pure oxygen (O2-GASIF), which enters the reactor at 200 °C and 25 bar. In the gasifier, restricted chemical equilibrium calculations take place at the selected gasification temperature, while the heat required for decomposition (Q) is provided from this reactor. Obtained products are sent to a separator block (SEPARATOR), where unconverted carbon and ash are removed (SLAG), thus simulating the formation of slag in the gasifier.

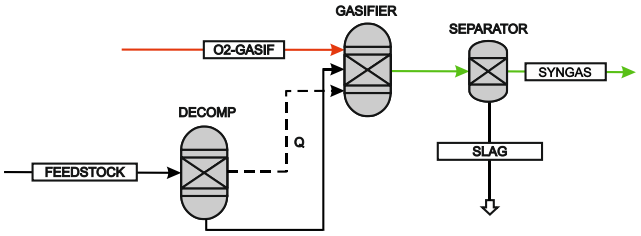

Figure 1. Aspen Plus gasification process flowsheet.

For the determination of the necessary oxygen flow rate for each simulation, equivalence ratio (ER) was used, while all calculations were performed in a Calculator block. The equivalence ratio for oxyfuel gasification is defined as:

$$ER = \frac{(O/F)}{(O/F)_{st}} \quad (2)$$

where O/F stands for the actual ratio of oxygen to fuel,

while $(O/F)_{st}$ stands for the stoichiometric ratio. Sensitivity analysis was performed for every raw material, with ER and gasification temperature being the parameters to be varied. Temperature was varied in the range of 1200 °C to 1500 °C, with 15 °C increments, while ER was varied in the range of 0.1 to 0.7, with 0.03 increments. A defined flowsheet configuration is set for the autothermal gasification regime; if the gasification reactor provides insufficient heat for decomposition (for example, when ER is too low, or when the material has a low heating value), the error is reported, and these results were not taken into consideration. Simulation results include the content of main syngas components (CO, H_2, CO_2, CH_4, and H_2O), while obtained data is used for the calculation of syngas *LHV*, carbon conversion, and cold gas efficiency (*CGE*). Carbon conversion and CGE are calculated from the following equations:

$$CONV = \frac{m_{c,in} - m_{c,out}}{m_{c,in}} \cdot 100(\%) \quad (3)$$

$$CGE = \frac{m_{syngas} \cdot LHV_{syngas}}{m_f \cdot LHV_f} \cdot 100(\%) \quad (4)$$

where $m_{c,in}$ and $m_{c,out}$ stand for carbon flow rate at gasifier inlet and outlet, m_{syngas} and m_f stand for syngas and feedstock mass flowrate, and LHV_{syngas} and LHV_f stand for syngas and feedstock LHV, respectively.

Artificial neural network modeling and optimization

Sensitivity analysis results are used as input data for the development of ANN for prediction of output parameters. MatLab's Neural Network Toolbox was used for the design of the neural network structure. A standard structure with one hidden layer was used, with a linear transfer function at the output layer and a tangent sigmoid function at the hidden layer. An algorithm was developed for the determination of the most suitable number of neurons in a hidden layer. The number of hidden neurons varied from 1 to 20, and the training process of each network was run 10 times with random initial values of weights and biases. The best topology was determined according to the coefficient of determination (R^2), Mean squared error (*MSE*), and mean absolute percentage error (*MAPE*) values. Bayesian regularization backpropagation algorithm was used for network training, where 60% of the data was used as training data, 20% as validation data, and 20% as test data. Each network consists of multiple inputs (ultimate analysis of feedstock material, moisture content, ER, and temperature) and singular output (syngas content of a selected component (CH_4, CO_2, CO, H_2, H_2O), syngas *LHV*, *CGE* or carbon conversion). Hence, 8 independent ANNs were developed.

Obtained functions are later used for process optimization for a given condition using a genetic algorithm function. As a result of the optimization procedure for a given feedstock material composition, the algorithm returns values for ER and gasification temperature. Therefore, the algorithm can be used for various problems, for example, in the maximization or minimization of specific component content in syngas, in adjusting of components ratio in syngas, in maximization of *CGE*, syngas heating value, or carbon conversion.

RESULTS AND DISCUSSION

Characteristics of investigated feedstock materials

As stated previously, materials of different origins were used in this study, to cover a wide range of elemental components compositions. It should be mentioned that some of the materials were completely unsuitable for the gasification process since the simulation reported errors for every combination of ER and temperature in sensitivity analysis. This is mainly due to high moisture content and low *LHV* value, which is typical for some MSW and biomass samples. The general characteristics of feedstock material which were suitable for gasification simulation are shown in Figure 2. It should be noted that the box plot for the chlorine content was not displayed due to its low content in all materials. Also, outliers in *LHV*, carbon, and sulfur content data correspond to coal samples used in this study.

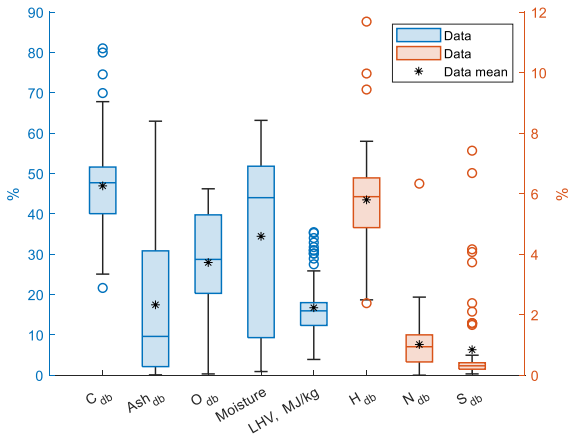

Figure 2. Box-plot representation of feedstock materials composition and LHV taken from literature; db stands for dry-basis composition.

Impact of operating conditions on entrained flow gasification

To analyze and discuss the relative impact of main operating conditions, ER, and temperature on the

oxyfuel EFG process, the results of a sensitivity study on a randomly selected feedstock material will be displayed. Surface plots for selected output parameters, mainly syngas composition and overall gasification parameters, are displayed in Figures 3 and 4. According to plots displayed in Figure 3, a nonlinear correlation between syngas composition and operating conditions can be observed. A crucial observation is that there is a distinctive range of operating parameter values for which H_2 and CO content are at maximum.

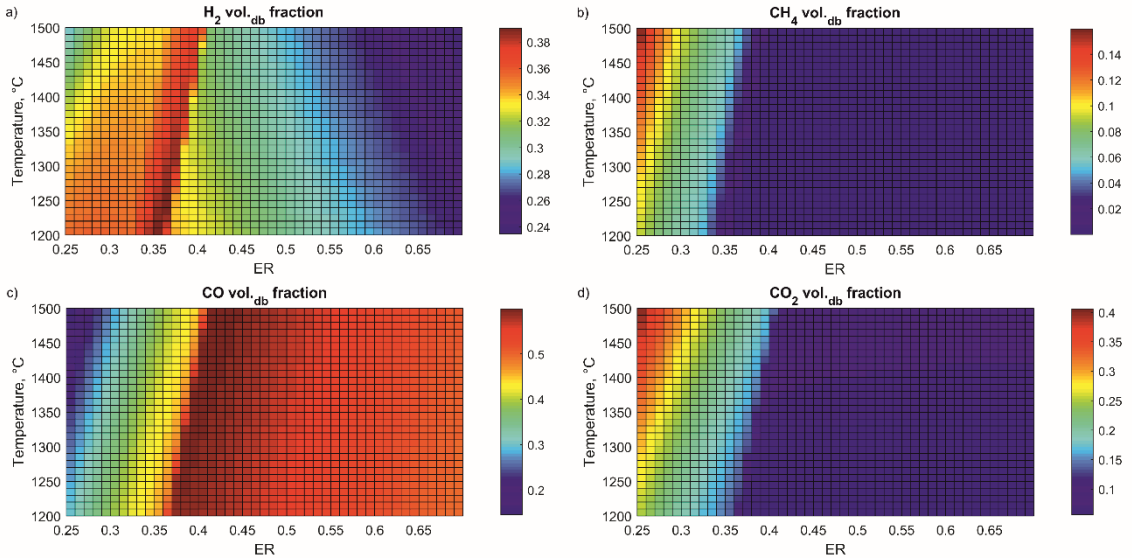

Figure 3. Dry-basis: (a) H_2 content, (b) CH_4 content, (c) CO content, (d) CO_2 content in syngas as a function of ER and gasification temperature.

Hydrogen content reaches maximum values in the ER range of 0.33–0.4 (Figure 3a), while lower temperatures favor hydrogen content increase. Maximum CO content is obtained in a similar ER range (Figure 3c), while a further increase of ER value slightly decreases CO content, with similar conclusions about temperature influence to be made. It can be assumed that the dominant reactions in the selected operating conditions range are partial oxidation and water-gas reactions. Methane content is significant at lower ER values (Figure 3b), where methanation and hydrogasification reactions are dominant. Methane and CO_2 content decrease with an increase of ER (Figures 3b and 3d), with a sharp decrease being in line with the area of maximum H_2/CO values.

Overall gasification efficiency is strongly dependent on the content of main syngas components, H_2 and CO, due to their high heating values. Cold gas efficiency increases with an increase in ER, with maximum CGE values being in the ER range of 0.33–0.4 and lower temperature area (Figure 4b). Complete carbon conversion is obtained after the 0.35 ER threshold, for all temperatures (Figure 4c). In general, higher gasification temperatures lower the conversion and *CGE*, due to the increase of necessary mixture sensible heat. It could be noted that the optimal operating conditions ensure complete carbon conversion with minimal consumption of gasifying agents. Syngas *LHV* follows a similar pattern, with the main difference being a significant decrease in high ER area (Figure 4a). However, higher ER results in higher overall gas yield, which explains the slight decrease in *CGE* values (Eq. (4) and Figure 4b).

Gasification kinetics in general is complex since the process takes place via a series of elementary reactions. However, it is stated in the literature that few global reactions, including only key components and interproducts, can be used for modeling purposes. Those reactions are given in Table 1 [43].

Table 1. Main gasification reactions.

Stoichiometry	Name
Char combustion	
$C+1/2O_2 \rightarrow CO$	Partial combustion
$C+O_2 \rightarrow CO_2$	Complete combustion
Char gasification	
$C+CO_2 \rightarrow 2CO$	Boudouard reaction
$C+H_2O \rightarrow CO+H_2$	Steam gasification
$C+2H_2 \rightarrow CH_4$	H_2 gasification
Homogenous	
$CO+1/2O_2 \rightarrow CO_2$	CO oxidation
$H_2+1/2O_2 \rightarrow H_2O$	H_2 oxidation
$CH_4+2O_2 \rightarrow CO_2+2H_2O$	CH_4 oxidation
$CO+H_2O \rightarrow CO_2+H_2$	Water-gas shift

Simulation results indicate that high hydrogen content corresponds to low water content in syngas, which can be attributed to the water-gas shift reaction, as well as the steam gasification reaction, where carbon is gasified with water vapor. At the area of complete carbon conversion, carbon gasification and oxidation no longer take place, which also causes hydrogen not to form via steam gasification reaction.

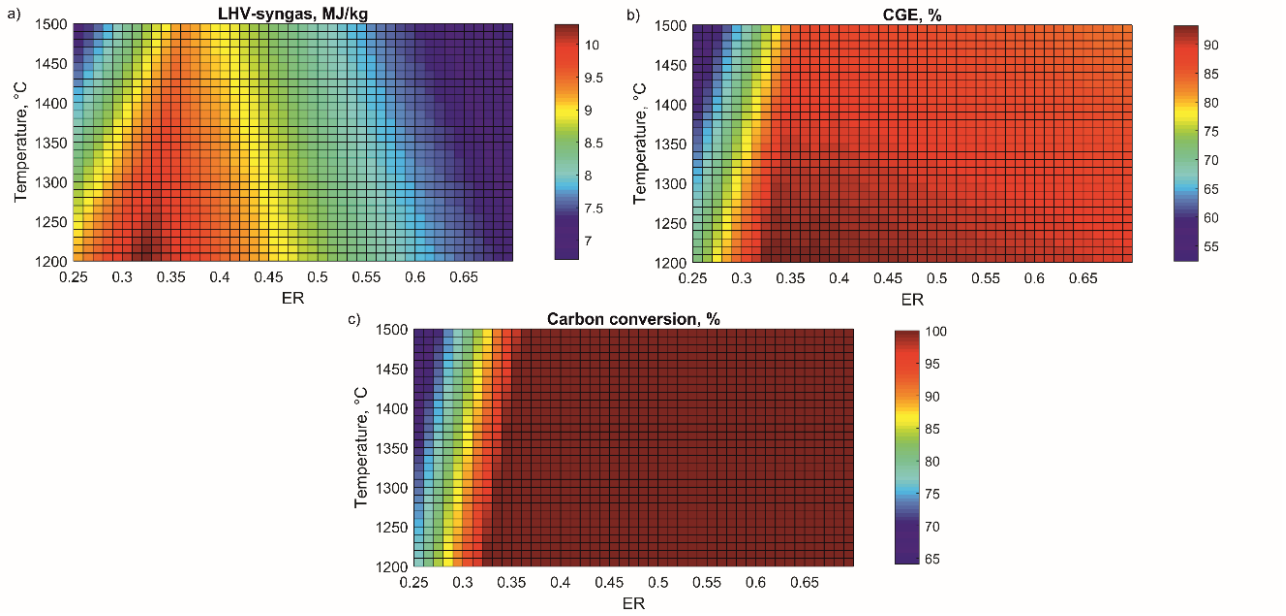

Figure 4. Overall gasification parameters, (a) syngas LHV, (b) CGE, (c) carbon conversion as a function of ER and gasification temperature.

Boudouard reaction is one of the most important reactions in the entire gasification mechanism, where carbon reacts with CO_2 while forming CO. This explains the decrease of CO content in the area of higher ER. At complete carbon conversion, the system stabilizes and no significant composition changes take place. Only homogenous reactions take place, primarily water-gas shift, while temperature and approximately equilibrium composition prohibit further reaction advancement. Also, it is important to highlight that methane and other hydrocarbons decompose at higher temperatures [13], which is why the obtained methane content is low.

Artificial neural networks

One neural network was developed for each output variable via the algorithm described in Materials and Methods. It should be noted that after initial runs, the number of input parameters decreases since chlorine and nitrogen contents in feedstock materials are very low and their impact on output variables should be negligible (due to the small quantity and inert nature of their gasification products). Likewise, ash is inert in the gasification process, thus, its impact is also neglected, resulting in 7 input parameters (carbon, hydrogen, oxygen, sulfur, and moisture contents, and ER and gasification temperature) for each output parameter. ANN performance and topology are shown in Table 2, while parity plots of some predicted and simulated values are shown in Figure 5. The remaining parity plots are given in Supplementary material, Figure S1.

The number of hidden neurons increases the prediction accuracy since the optimal number of neurons was close to 20, while coefficients of determination values were above 0.99 for all instances. The impact of hidden neurons' number on the coefficient of determination for each neural network is given in Supplementary material, Figures S2 and S3. High accuracy is also confirmed by low MSE and MAPE values. It should be noted that simulated values of certain values are close to zero for a wide range of operating parameters, thus resulting in a relatively high MAPE value, even though overall prediction accuracy is high.

Table 2. Artificial neural network structure and prediction accuracy.

Each output neuron	Hidden neurons	R^2	MAPE %	MSE
H_2	19	0.9938	4.3858	$4.7553 \cdot 10^{-5}$
CO	19	0.9988	13.6318	$4.4521 \cdot 10^{-5}$
CH_4	19	0.9987	60.3509	$2.74339 \cdot 10^{-6}$
CO_2	20	0.9968	16.8125	$2.9776 \cdot 10^{-5}$
H_2O	20	0.9984	7.0330	$6.6187 \cdot 10^{-5}$
Syngas LHV	20	0.9997	0.4967	0.0035
CGE	20	0.9989	1.3559	0.6355
Carbon conversion	20	0.9994	0.2970	0.1951

To quantify the impact of input variables on syngas composition and overall gasification parameters, Yoon's interpretation method was used [44]. Obtained results are displayed in Table 3. It can be noted that the equivalence ratio has a higher general impact on syngas composition and overall gasification efficiency than temperature, while carbon and moisture content impact the syngas composition the most. Results on the relative importance of ER and gasification temperature are in line with sensitivity analysis results displayed previously.

Since developed neural network models show

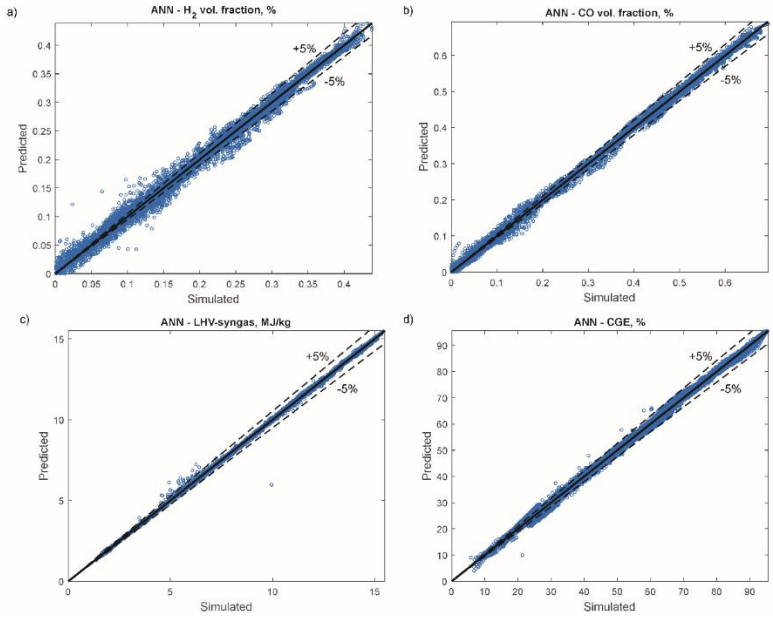

Figure 5. Simulated and predicted data on (a) H_2 content, (b) CO content, (c) syngas LHV, and (d) CGE, according to the developed ANN model.

Table 3. The relative impact of input parameters on output parameters in the EFG process.

	ER	T, °C	C	H	O	Moisture
H_2	38.0±12.5	-4.3±0.5	13.6±2.8	1.6±6.4	6.3±9.1	-17.4±4.5
CO	38.7±7.2	-3.8±0.6	11.5±4.2	3.0±7.8	4.0±3.8	-15.3±8.5
CH_4	-49.9±6.2	4.3±0.5	-12.4±1.6	5.7±2.7	-1.6±2.5	10.1±5.6
CO_2	-21.2±6.7	3.8±1.0	-7.5±7.8	-9.7±5.0	2.1±7.2	12.0±8.6
H_2O	-36.1±8.4	4.1±0.6	-16.3±4.3	-2.8±4.9	-2.0±4.4	23.3±3.1
Syngas LHV, MJ/kg	7.7±11.3	-3.6±0.9	4.5±4.4	20.0±5.0	-2.7±4.9	-14.3±6.6
CGE, %	4.2±5.3	-0.6±0.8	9.4±5.5	-9.7±17.3	-3.9±11.8	-7.1±6.6
Carbon conversion, %	39.7±7.4	-1.7±0.6	-1.3±2.9	7.5±4.1	9.5±3.7	9.3±5.3

good agreement between simulated and predicted data, they could be further used for optimization purposes. Two optimization problems were tested; obtaining the maximum hydrogen fraction in syngas and obtaining of maximum CGE for a given feedstock material. A genetic algorithm was used for optimization on each feedstock material, with ER and gasification temperature as output parameters. Parity plots on simulated (based on sensitivity analysis results) and predicted (optimization) hydrogen fraction and CGE are shown in Figure 6.

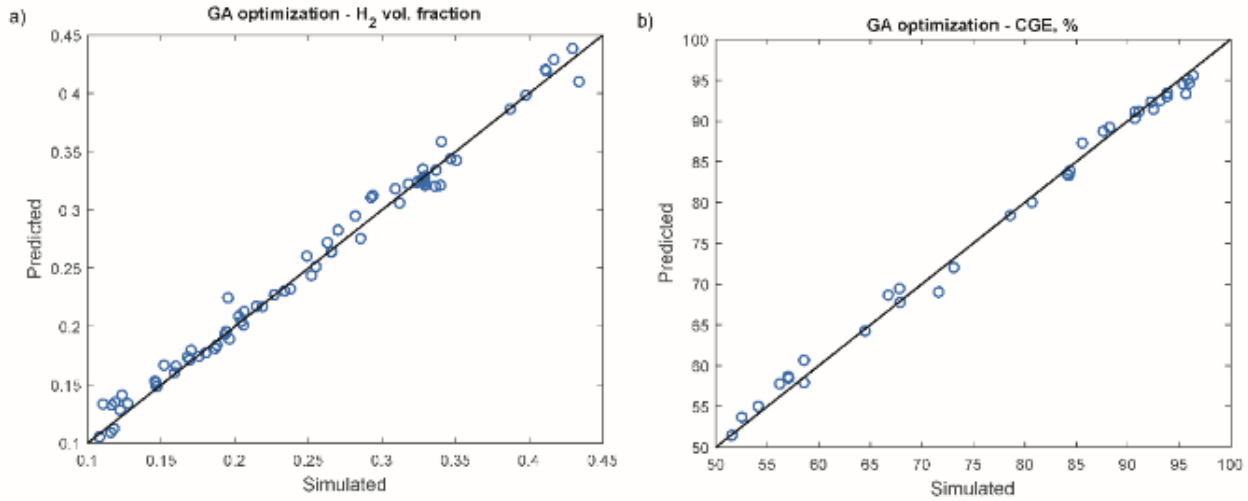

Figure 6. Predicted and simulated; (a) H_2 content and (b) CGE according to optimization procedure.

The obtained optimization results are in accordance with sensitivity analysis results. It should be noted that ER and temperature are in this case continuous variables, contrary to sensitivity analysis, which could lead to slight deviation of results. Temperatures corresponding to optimal operating conditions are close to the minimal gasification temperature of 1200 °C, while mean ER values are 0.35 for hydrogen optimization and 0.41 for CGE optimization.

In general, this approach contributes to a better understanding of EFG process kinetics, while developed ANN models can be used for quick prediction of gasification output parameters for a given feedstock. Obtained syngas composition can be further used to facilitate gasification-based process simulation since complex three-phase calculations are bypassed. Also, models can be used for process optimization i.e. obtaining the optimal operating conditions for a specified goal.

CONCLUSION

An integrated ANN and Aspen Plus gasification model was used for the investigation of entrained flow gasification kinetics. Various feedstock materials, mainly waste, RDF, coal, and biomass were used to obtain a wide range of input material elemental compositions. For each feedstock material, sensitivity analysis on EFG in Aspen Plus was performed, for different equivalence ratios and temperatures, and obtained results were used in ANN development. Single layer ANNs with an adjustable number of neurons were developed for every output variable (syngas components fractions, cold gas efficiency, syngas lower heating value, and carbon conversion), with high prediction accuracy (R^2>0.99). All models consist of a high number of hidden neurons (19–20). Also, the general impact of ER and temperature, as well as feedstock material composition on output parameters was determined and discussed. The highest gasification efficiencies are obtained at lower temperatures, just above ash melting temperatures, and in a narrow range of ER, typically 0.35–0.45, depending on feedstock material composition. In this ER range, the highest H_2 content and moderate CO content are obtained, resulting in the highest syngas heating value. Further increase of ER does not have a significant effect on syngas composition. Obtained models can be used for optimization problems, where two desired goals were successfully tested; determination of optimal combination of ER and temperature for maximization of syngas hydrogen content and cold gas efficiency. For investigated materials, mean optimal parameters are temperature of 1200 °C and ER of 0.41 and 0.35 for cold gas efficiency and hydrogen content, respectively. This combined ANN and simulation approach allows for quick and accurate prediction of EFG efficiency and syngas composition, thus providing essential information for the design and development of gasification processes.

ACKNOWLEDGEMENTS

The authors would like to thank the Ministry of Education, Science and Technological Development of the Republic of Serbia, Project No. 451-03-65/2024-03/200134.

REFERENCES

[1] H. Ritchie, P. Rosado, M. Roser, Energy Production and Consumption, https://ourworldindata.org/energy-production-consumption, [accessed 7 May 2024].

[2] IEA, World Energy Outlook 2022, https://www.iea.org/reports/world-energy-outlook-2022 . [accessed 7 May 2024].

[3] M.N. Dudin, E.E. Frolova, O.V. Protopopova, O. Mamedov, S.V. Odintsov, 6 (2019) 1704. https://doi.org/10.9770/jesi.2019.6.4(11).

[4] C.-F. Schleussner, J. Rogelj, M. Schaeffer, T. Lissner, R. Licker, E.M. Fischer, R. Knutti, A. Levermann, K. Frieler, W. Hare, Nat Clim Chang 6 (2016) 827–835. https://doi.org/10.1038/nclimate3096.

[5] L. Mundaca, L. Neij, A. Markandya, P. Hennicke, J. Yan, Appl Energy 179 (2016) 1283–1292. https://doi.org/10.1016/j.apenergy.2016.08.086.

[6] H.B. Goyal, D. Seal, R.C. Saxena, 12 (2008) 504–517. https://doi.org/10.1016/j.rser.2006.07.014.

[7] V. Kirubakaran, V. Sivaramakrishnan, R. Nalini, T. Sekar, M. Premalatha, P. Subramanian, 13 (2009) 179–186. https://doi.org/10.1016/j.rser.2007.07.001.

[8] V. Tola, A. Pettinau, Appl Energy 113 (2014) 1461–1474. https://doi.org/10.1016/j.apenergy.2013.09.007.

[9] J. Parraga, K.R. Khalilpour, A. Vassallo, 92 (2018) 219–234. https://doi.org/10.1016/j.rser.2018.04.055.

[10] R. Rauch, J. Hrbek, H. Hofbauer, Wiley Interdiscip Rev Energy Environ 3 (2014) 343–362. https://doi.org/10.1002/9781118957844.ch7.

[11] A. Molino, S. Chianese, D. Musmarra, 25 (2016) 10–25. https://doi.org/10.1016/j.jechem.2015.11.005.

[12] M. Lapuerta, J.J. Hernández, A. Pazo, J. López, 89 (2008) 828–837. https://doi.org/10.1016/j.fuproc.2008.02.001.

[13] U. Arena, 32 (2012) 625–639. https://doi.org/10.1016/j.wasman.2011.09.025.

[14] J.J. Hernández, G. Aranda-Almansa, A. Bula, 91 (2010) 681–692. https://doi.org/10.1016/j.fuproc.2010.01.018.

[15] M. Puig-Arnavat, J.C. Bruno, A. Coronas, 14 (2010) 2841–2851. https://doi.org/10.1016/j.rser.2010.07.030.

[16] E. Henrich, F. Weirich, Environ Eng Sci 21 (2004) 53–64. https://doi.org/10.1089/109287504322746758.

[17] T. Xu, Y. Wu, S. Bhattacharya, Int J Min Sci Technol 31

(2021) 473–481. https://doi.org/10.1016/j.ijmst.2021.03.001.

[18] F. Qian, X. Kong, H. Cheng, W. Du, W. Zhong, Ind Eng Chem Res 52 (2013) 1819–1828. https://doi.org/10.1021/ie301630x.

[19] M. Vascellari, R. Arora, C. Hasse, 118 (2014) 369–384. https://doi.org/10.1016/j.fuel.2013.11.004.

[20] G.-S. Liu, H.R. Rezaei, J.A. Lucas, D.J. Harris, T.F. Wall, 79 (2000) 1767–1779. https://doi.org/10.1016/S0016-2361(00)00037-5.

[21] A. Tremel, H. Spliethoff, 107 (2013) 170–182. https://doi.org/10.1016/j.fuel.2013.01.062.

[22] M. Vascellari, D.G. Roberts, D.J. Harris, C. Hasse, 152 (2015) 58–73. https://doi.org/10.1016/j.fuel.2015.01.038.

[23] I. Adeyemi, I. Janajreh, Renew Energy 82 (2015) 77–84. https://doi.org/10.1016/j.renene.2014.10.073.

[24] M.A. Kibria, P. Sripada, S. Bhattacharya, 196 (2020) 117073. https://doi.org/10.1016/j.energy.2020.117073.

[25] M. Al-Zareer, I. Dincer, M.A. Rosen, 115 (2016) 1–18. https://doi.org/10.1016/j.cherd.2016.09.009.

[26] M. Pérez-Fortes, A.D. Bojarski, E. Velo, J.M. Nougués, L. Puigjaner, 34 (2009) 1721–1732. https://doi.org/10.1016/j.energy.2009.05.012.

[27] Y. Lu, Z. Li, M. Zhang, C. Huang, Z. Chen, Energy Convers Manag 245 (2021) 114627. https://doi.org/10.1016/j.enconman.2021.114627.

[28] Z. Dai, X. Gong, X. Guo, H. Liu, F. Wang, Z. Yu, 87 (2008) 2304–2313. https://doi.org/10.1016/j.fuel.2007.12.005.

[29] D. Barba, M. Prisciandaro, A. Salladini, G.M. Di Celso, 90 (2011) 1402–1407. https://doi.org/10.1016/j.fuel.2010.12.022.

[30] Ö.Ç. Mutlu, T. Zeng, Chem Eng Technol 43 (2020) 1674–1689. https://doi.org/10.1002/ceat.202000068.

[31] M. Ozonoh, B.O. Oboirien, A. Higginson, M.O. Daramola, Renew Energy 145 (2020) 2253–2270. https://doi.org/10.1016/j.renene.2019.07.136.

[32] H.O. Kargbo, J. Zhang, A.N. Phan, Appl Energy 302 (2021) 117567. https://doi.org/10.1016/j.apenergy.2021.117567.

[33] M. Puig-Arnavat, J.A. Hernández, J.C. Bruno, A. Coronas, Biomass Bioenergy 49 (2013) 279–289. https://doi.org/10.1016/j.biombioe.2012.12.012.

[34] D. Baruah, D.C. Baruah, M.K. Hazarika, Biomass Bioenergy 98 (2017) 264–271. https://doi.org/10.1016/j.biombioe.2017.01.029.

[35] R. Mikulandrić, D. Lončar, D. Böhning, R. Böhme, M. Beckmann, Energy Convers Manag 87 (2014) 1210–1223. https://doi.org/10.1016/j.enconman.2014.03.036.

[36] S. Ascher, W. Sloan, I. Watson, S. You, Appl Energy 320 (2022) 119289. https://doi.org/10.1016/j.apenergy.2022.119289.

[37] F. Kartal, U. Özveren, 209 (2020) 118457. https://doi.org/10.1016/j.energy.2020.118457.

[38] S. Safarian, S.M.E. Saryazdi, R. Unnthorsson, C. Richter, 213 (2020) 118800. https://doi.org/10.1016/j.energy.2020.118800.

[39] J. Chen, J. Liang, Z. Xu, E. Jiaqiang, Energy Convers Manag 226 (2020) 113497. https://doi.org/10.1016/j.enconman.2020.113497.

[40] H. Shahbeik, W. Peng, H.K.S. Panahi, M. Dehhaghi, G.J. Guillemin, A. Fallahi, H. Amiri, M. Rehan, D. Raikwar, H. Latine, 167 (2022) 112833. https://doi.org/10.1016/j.rser.2022.112833.

[41] M. Shahbaz, T. Al-Ansari, M. Inayat, S.A. Sulaiman, P. Parthasarathy, G. McKay, 134 (2020) 110382. https://doi.org/10.1016/j.rser.2020.110382.

[42] A. Ozyuguran, A. Akturk, S. Yaman, 214 (2018) 640–646. https://doi.org/10.1016/j.fuel.2017.10.082.

[43] A. Gómez-Barea, P. Ollero, B. Leckner, 103 (2013) 42–52. https://doi.org/10.1016/j.fuel.2011.04.042.

[44] Y. Yoon, G. Swales Jr, T.M. Margavio, 44 (1993) 51–60. https://doi.org/10.1057/jors.1993.6.

DARIO BALABAN[1,2]
JELENA LUBURA[1]
PREDRAG KOJIĆ[1]

[1]Univerzitet u Novom Sadu, Tehnološki fakultet Novi Sad, Novi Sad, Srbija

[2]Univerzitet u Istočnom Sarajevu, Tehnološki fakultet Zvornik, Zvornik, Republika Srpska, Bosna i Hercegovina

INTEGRISANI MODEL ZASNOVAN NA NEURONSKIM MREŽAMA I ASPENPLUS SOFTVERU ZA ISPITIVANJE KINETIKE GASIFIKACIJE U ZAHVAĆENOM TOKU ČESTICA

Gasifikacija u zahvaćenom toku čestica predstavlja razvijenu tehnologiju, međutim, glavna prepreka u projektovanju procesa je složen mehanizam gasifikacije, s obzirom da se više fenomena na ekstremnim procesnim uslovima odvija istovremeno. Ova studija je fokusirana na integrisani pristup pomoću termodinamike i veštačkih neuronskih mreža (ANN) za ispitivanje kinetike gasifikacije u zahvaćenom toku čestica. Podaci o 102 sastava sirovina su korišteni za simulaciju gasifikacije u AspenPlus softveru, gde je analiza osetljivosti izvršena za različite ekvivalentne odnose (0.1–0.7) i gasifikacione temperature (1200–1500 °C). Za analizirane sirovine postoji optimalni opseg ekvivalentnog odnosa (obično 0.3–0.4), čime se maksimizije efikasnost gasifikacije. Dobijeni rezultati su korišteni za razvoj ANN za svaku izlaznu promenljivu (sastav singasa, efikasnost, toplotna moć i konverzija ugljenika). Matlab algoritam je korišten za određivanje optimalnog broja neurona (u opsegu od 1–20) za svaku ANN. Visoka vrednost R^2 (>0.99) za sve modele ukazuje na dobro poklapanje između simuliranih i predviđenih vrednosti. Optimizacione studije bazirane na genetičkom algoritmu za maksimizaciju sadržaja vodonika i hladne efikasnosti gasa rezultuju srednjim ER vrednostima od 0.35 i 0.41, respektivno, na temperaturi od 1200 °C. Yoon-ova metoda interpretacije je korištena za kvantifikaciju relativnih uticaja svake ulazne promenljive na sadržaj singasa i efikasnost gasifikacije. Predloženi pristup predstavlja moćan alat koji može da ubrza istraživanje procesa gasifikacije u zahvaćenom toku čestica i projektovanje procesa.

Ključne reči: singas; optimizacija; simulacija; mašinsko učenje.

NAUČNI RAD